Research Article

BROAD PHASE RESPONSE UNIT CELL AND HIGH GAIN REFLECARRAY ANTENNA DESIGN WITH CIRCLE-MINKOWSKI STRUCTURES

Authors: Bülent Urul iD

To link to this artice: https://dergipark.org.tr/tr/pub/ijeir/archive

BROAD PHASE RESPONSE UNIT CELL AND HIGH GAIN REFLECARRAY ANTENNA DESIGN WITH CIRCLE-MINKOWSKI STRUCTURES

Bülent Urul[1]*

[1]Isparta Applied Sciences University, Vocational School of Technical Science, Electronics and Automation Department, Isparta, Turkey.

*Corresponding Author: bulenturul@isparta.edu.tr

ABSTRACT: In this study, it is aimed to increase the phase responses of the obtained unit cells by using the fractal structures nested together. Then, the effect of these obtained broad phase-response unit cells on the antenna gain is examined by using them as reflective elements on the reflect array antenna. For this purpose, 3 different structures are designed: the circle, the Minkowski used in the circle, and the unit cells obtained by rotating the Minkowski structure in the circle. The phase response of the first designed circle structure could not meet the phase requirement for a whole band, and a phase response of 280° is obtained. Then, in the second stage, the Minkowski structure is designed in the designed circle, and a phase response of 329° is obtained in this structure. Finally, a structure sufficient for the entire phase response is obtained by rotating the Minkowski structure in the circle between $0^o - 30^o$. A unit cell with a wide phase response and a 11.7 dBi horn antenna and reflect array antenna are designed. The gain of the designed reflect array antenna has increased by 91% compared to the horn antenna and has been obtained as 22.4 dBi. With this result, it has been revealed that the phase response can be increased by using fractal structures together and especially by rotating the structures, and with this method, high-gain reflect array antennas with broadband phase response can be designed.

Keywords: Fractal structures, Reflect array antenna, Antenna gain.

1. INTRODUCTION

Reflect array antennas (RAA) are antenna structures that significantly demonstrate effectiveness in communication technologies, wireless communication systems and satellite communications. These structures basically consist of a horn antenna as a feed antenna and multiple reflective microstrip structures placed on a flat ground. As it is known, microstrip antennas are highly preferred by engineers and researchers due to their low cost, easy production, thin and planar production capabilities, and so they are the subject of many studies[1-3]. Likewise, horn antennas are antennas with high directivity and wide bandwidth. RAA which can normally be produced as parabolic, can be produced in a thin planar way by combining these superior properties of horn and microstrip antennas.

Fractal structures such as Penta, Koch-triangle, and Minkowski are frequently used as reflective unit cells used in RAA. Fractal geometries are characterized by the use of the same geometry in a certain ratio of small and large versions. That is, a particular shape is scaled and repeated several times to create the fractal structure used. When creating fractal structures, the fractal

shape is derived in an iterative procedure based on the scaling factor of an initial shape, the fractal generator, the size of the shape to scale, and the number of iterations. The application of fractal geometries to conventional antennas increases the antenna performance, thus reducing the overall size of the structure used [4-6]. Because of these properties of fractal structures, it is often preferred in the design of reflective array antennas and phased array antennas.

However, bandwidth limitation is a major problem in design of RAA, which is due to the narrow bandwidth of the radiating elements themselves. Various methods have been suggested in the literature to increase the bandwidth of the radiating elements, such as using patch elements of different structure. Single-layer wideband reflect arrays have been studied by using multi-resonant radiating elements. Efforts have also been made to improve bandwidth using single-layer broadband reflector arrays, multi-resonant radiation elements, or using sub-wavelength elements. With these applications, the bandwidth can be increased even in single-layer structures [7-13].

The working principle of RAAs is to reflect the incoming wave from the surface of the reflective array elements and direct it to a desired point. Sometimes the source is placed in the center directly opposite the reflective antenna, and sometimes it can be placed as an offset. The biggest advantage of reflective array antennas over normal reflective antennas is that they can be placed on a flat surface. Therefore, it has the advantage of easy production [14,15]. However, in order to reflect the incoming beam to the desired point, it must first be determined how much reflection phase is required at which point on the antenna. The patch reflective elements then need to be placed on the planar antenna surface. By changing the values of each element placed on the surface, such as size, shape, angle of rotate, the reflection phase values required by each point on the antenna are obtained. This process is called phase compensation process[16,17].

In this article, first a circular reflector is designed as a reflector array element, and then the Circle-Minkowski shape obtained by removing the Minkowski shape, which is a fractal structure, from the circle by etching is designed. The Minkowski fractal reflective array cell is used by many researchers in their work. While the patch size is sometimes properly kept constant during the design phase, the reflection phase control is accomplished by varying the scaling factor n. In our study, the phase compensation of the Minkowski cell was achieved by changing the scaling ratio n and accordingly the patch size t and the indentation value s. In addition, the effect of the circle used on the reflection phase was evaluated. As a result of all the operations, unit cell size values that can provide the phase requirements at all points of the RAA have been found. Finally, the RAA gain values obtained after appropriate phase compensation are obtained.

2. METHODOLOGY

2.1. Reflective unit cell designs

2.1.1. Circular unit cell design

In this part, 3 different designs are being made with 11GHz center frequency. The first design is only in the form of a circle, as seen in Figure 1. All studies are designed and simulated with the help of CST electromagnetic simulation program. For the simulation setup in the simulation program, open (add space) is selected for all axes as boundary conditions. In addition, the number of cells for each wavelength is 10, the accuracy is -60 dB.
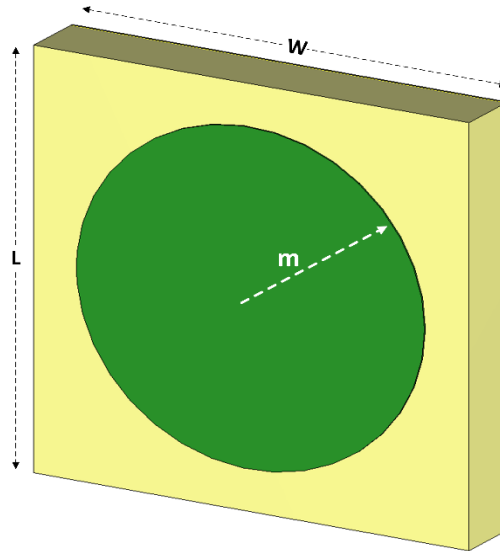
Figure 1. Circle reflective unit cell

Here, Taconic RF-35 (lossy) substrate is preferred as substrate. The loss tangent of the substrate is 0.0018 for the 11 GHz frequency and its electrical permeability is 3. In order to maximize reflection, the ground layer is covered with copper. The patch used on the substrate is preferred as copper. The radius of the circle structure used varies in the range of 2-5 mm. Circle unit cell parameters are given in Table 1.

Table 1. Circle unit cell design parameters

Parameters	Unit (mm)
m	Between 2-4.8
Substrate length (L)	10
Substrate width (W)	12
Substrate thickness	1.5
Copper thickness	0,035

After the design process, the circular reflective unit cell is simulated by the electromagnetic simulation program and the phase correspondence values according to the circle radius are obtained as shown in Figure 2.
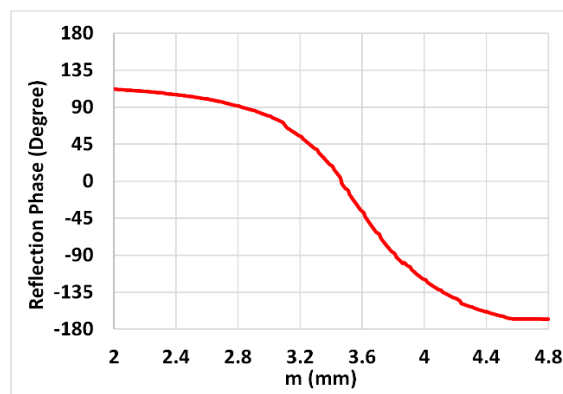

Figure 2. Phase response plot corresponding to m for a circle reflective unit cell

When the graph in Figure 2 is examined, it is seen that the reflection phase angle values corresponding to the m value vary between 112° and -168° and a total phase response of 280° can be obtained.

2.1.2. Circle-Minkowski unit cell design (Without rotation)

In the second reflective unit cell design, as seen in Figure 3, the Minkowski structure is extracted from the circle shape by etching.
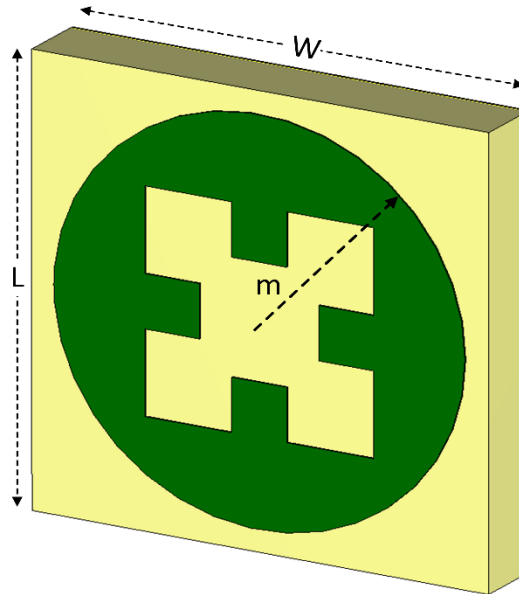

Figure 3. Unit cell with Minkowski structure etched from the circle

In Figure 3, the unit cell structure with the Minkowski structure etched from the circle is seen. In this design, the change of the reflection phase angle is examined by keeping the basic parameters constant and changing the parameters of the circle and Minkowski structures.

The shape parameters of the Minkowski structure are shown in Figure 4. There are 3 different cases for m, t and s values. Two of these parameters should be kept constant, one should be changed, 3 different simulation processes should be performed and phase responses should be evaluated. Accordingly, firstly, the unit cell is simulated by keeping the shape parameters of the Minkowski structure, t and s constant, and changing the circle radius (m). But here, in order that the radius of the circle is not smaller than the Minkowski shape, the dimensions of the Minkowski structure should be as small as possible and the chosen circle radius should be chosen in accordance with the Minkowski dimensions. Accordingly, the relation given in Equation 1 between the indentation s and the width t, used on the Minkowski structure, is taken into account. The value of n is preferred in the range of 0 to 1. Accordingly, t = 2 mm in Figures 3 and 4 is kept constant at s = 0.53mm (n=0.8) and the graph in Figure 5 is obtained by changing the circle radius between 2-4.8mm.

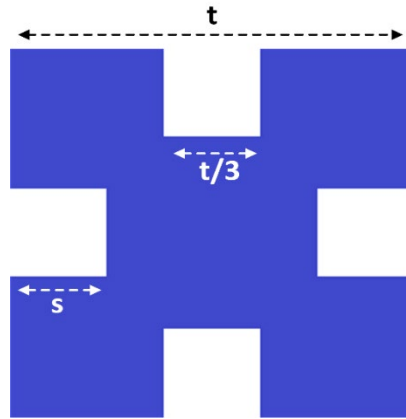$$n = \frac{s}{t/3} \qquad 0 \leq n \leq 1 \tag{1}$$
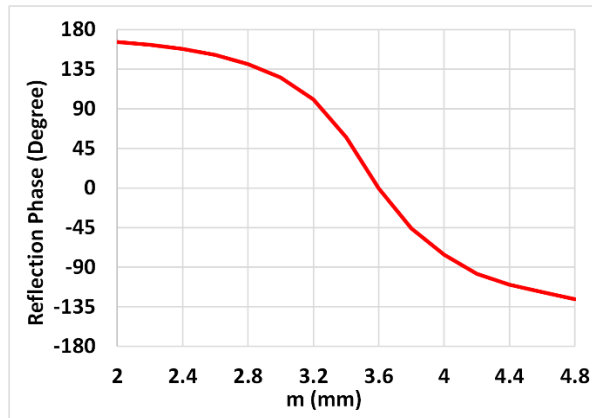
Figure 4. Minkowski structure

Figure 5. Phase response plot corresponding to m value for Circle-Minkowski reflective unit cell (m=2-4.8 mm, t=2 mm, s=0.53mm)

When Figure 5 is examined, when the circle radius m value increases for the Circle-Minkowski structure, the reflection phase value decreases, and on the other hand, a phase response of 294° between $+126^{o}$ and -168° is obtained for all angle values. appears to be unavailable.

In the second case, the effect of changing the t minkowski width on the reflection phase value is examined by keeping the m value, which is the circle radius, and the s minkowski indentation value constant. Accordingly, the unit cell is simulated according to the change of t value by keeping it constant at m = 4.5 mm and s=0.53 mm (n = 0.8 mm) and Figure 6 is obtained.
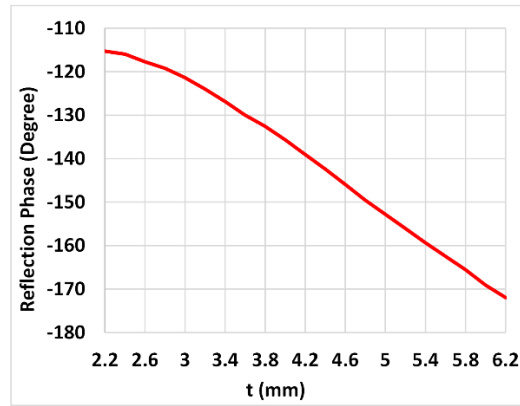
Figure 6. Phase response plot corresponding to the m value for the Circle-Minkowski reflective unit cell (m=4.5 mm, t=2.2-6.2 mm, s=0.53 mm)

When Figure 6 is examined, it can be seen from the graph that a phase equivalent can be obtained between about -115° and -172°, and the reflection phase value decreases as the t value increases.

In the third case, the effect of changing the s value, which is the indentation size, on the phase response is examined by keeping the m and t values constant. The unit cell is simulated by keeping m = 4.5 mm and t = 3 mm constant and changing the s value in the range of 0.05-0.85 mm. Accordingly, the graph in Figure 7 is obtained.
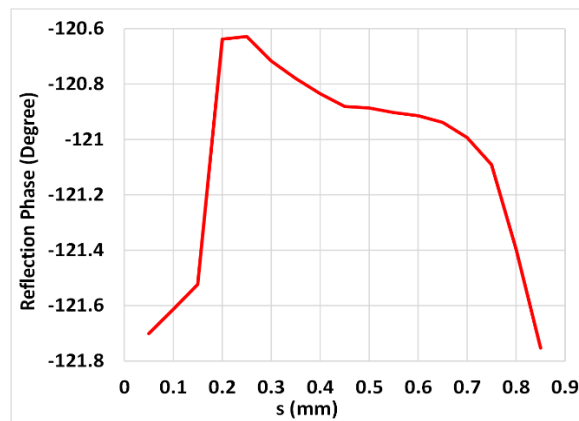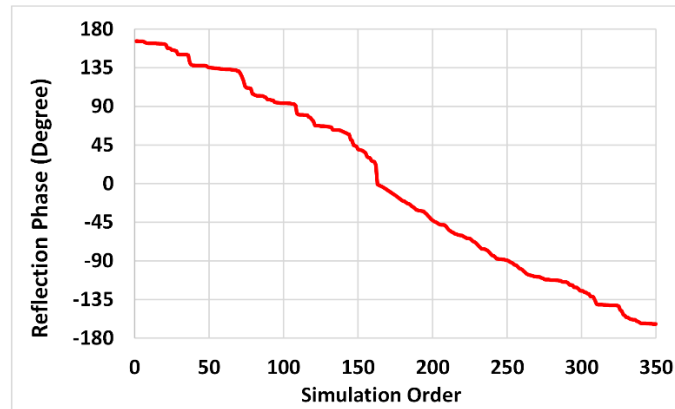

Figure 7. Phase response plot corresponding to m value for Circle-Minkowski reflective unit cell (m=4.5 mm, t=2-6.2 mm, s=0.53mm)

When Figure 7 is examined, it is seen that there are very small irregular changes in the phase value, and the phase angle varies between $-120,62^o$ and $-121,7^o$. Accordingly, it can be said that the s indentation value has a very small effect on the phase angle. According to all these data, the common usage and changes of m, t and s values and the unit cell given in Figure 3 are simulated according to the simulation parameters given in Table 2.

Table 2. Circle-Minkowski structure design parameters

Parameters (mm)		
m	**t**	**s**
4.8-4.5	6.2-2.0	0.05-0.85
4.4-4.0	5.5-2.0	0.05-0.85
3.9-3.2	4.4-2.0	0.05-0.85
3.1-2.3	3.2-2.0	0.05-0.85

While preparing Table 2, it should be taken into account that the value of m cannot be less than the value of t. The simulation process was performed according to these parameters and Figure 8 is obtained. In addition, since the phase response will depend on the m, t and s values at the same time, Figure 8 is given as the phase response graph corresponding to the simulation number.

Figure 8. Phase response plot for Circle-Minkowski reflective unit cell

When Figure 8 is examined, it is seen that the phase response varies between $+166^o$ and -163° and there is a phase gap of 31° where no phase response can be obtained. Therefore, this means that there are points on the substrate where phase response cannot be obtained while designing the reflective array.

2.1.3. Circle-Minkowski unit cell design (With rotation)

The third step in the design of the reflective unit cell is to simulate the circle-Minkowski structure by rotating it between 0°-30° as seen in Figure 9. The simulation parameters are the same as in the previous step and the simulation process was performed by only rotating.
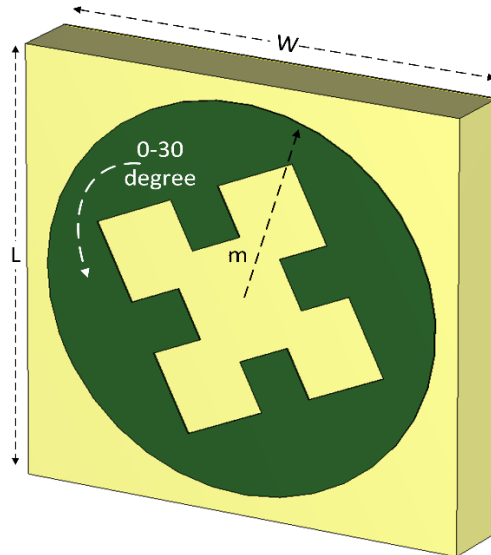
Figure 9. Circle-Minkowski reflective unit cell (With rotation)

A total of 3500 simulations were performed for the parameters used in Table 2 and for 10 angle values between 0°-30° and the reflection phase graph corresponding to these parameters is given in Figure 10. As can be seen in Figure 10, the phase response rotation of the unit cell spreads over a wider range, ranging from $+180^o$ to -180°. This ensures that the phase response can be obtained for each point on the antenna while designing the reflective array antenna and the corresponding unit cells can be placed at all points.

Figure 10. Phase response plot for Circle-Minkowski reflective unit cell (With Rotation)

2.2. Reflect array antenna design

RAAs are generally designed in 3 different structures as circle, square and rectangular incoming plane waves. However, the working process of all of them is based on the phase delay principle after the wave coming to the antenna surface illuminated by a source placed in the center or offset, after it is reflected again. The top and side view structure of the RAA is given in Figure 11.
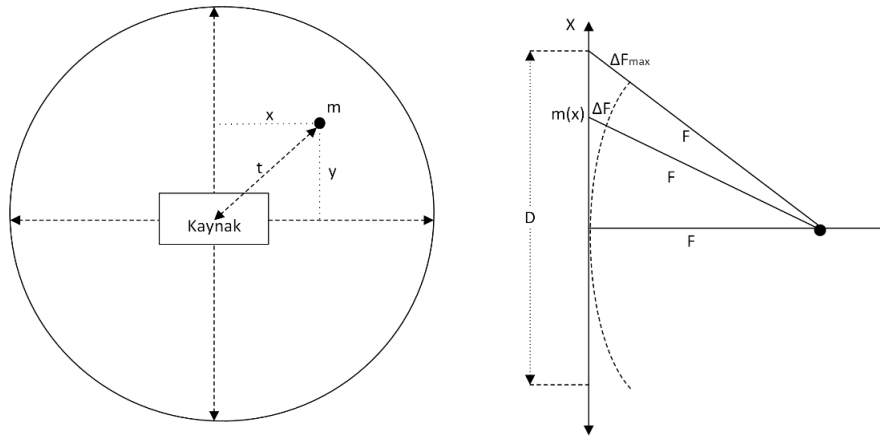
Figure 11. Top and side view for reflective array antenna (with Calculation parameters)

In the reflective array antenna, the basic structure of which is given in Figure 11, the D distance is the diameter of the antenna, the F distance is the distance between the source and the antenna, the ΔF distance is the path length that must be compensated by the phase delay for the reflective element at any point, and the distance ΔF_{max} also represents the maximum amount of path that needs to be compensated at the corner of the antenna. The m in Figure 10 indicates the coordinate of the unit cell placed on the antenna and using Equation 2, the distance of the unit cell to the origin point is calculated.

$$t = \sqrt{x^2 + y^2} \qquad (2)$$

The distance ΔF, which represents the amount of path to be compensated at the point where the unit cell is located, can be calculated using Equation 3. Here, the ΔF path difference is calculated by subtracting the distance of the unit cell from the source connected to F and t, from the source to the origin point.

$$\Delta F = \sqrt{F^2 + t^2} - F \qquad (3)$$

The required phase delay amount (φ) placed at any m point of the antenna can be calculated using Equation 4.

$$\varphi = -\beta(\Delta Fmax - \Delta F) \qquad (4)$$

β, used in Equation 4, represents the path constant of the medium and is expressed by $\beta = -2\pi\frac{f}{c}$. Therefore, Equation 4 can also be expressed as Equation 5. Here, f represents the frequency and c represents the speed of light.

$$\varphi = -2\pi\frac{f}{c}(\Delta Fmax - \Delta F) \qquad (5)$$

Using these equations and antenna structure, the phase delay requirement at each point on the RAA is calculated. Then, using the simulation values in Section 2.1.1-2, the unit cell structures that provide the phase requirement of each point on the antenna are placed on the antenna. After the correct sized unit cell structures are placed on the antenna, a horn antenna with a center frequency of 11 GHz is placed on the RAA as shown in Figure 12. In addition, the shape and dimensions of the horn antenna used are given in Figure 13.
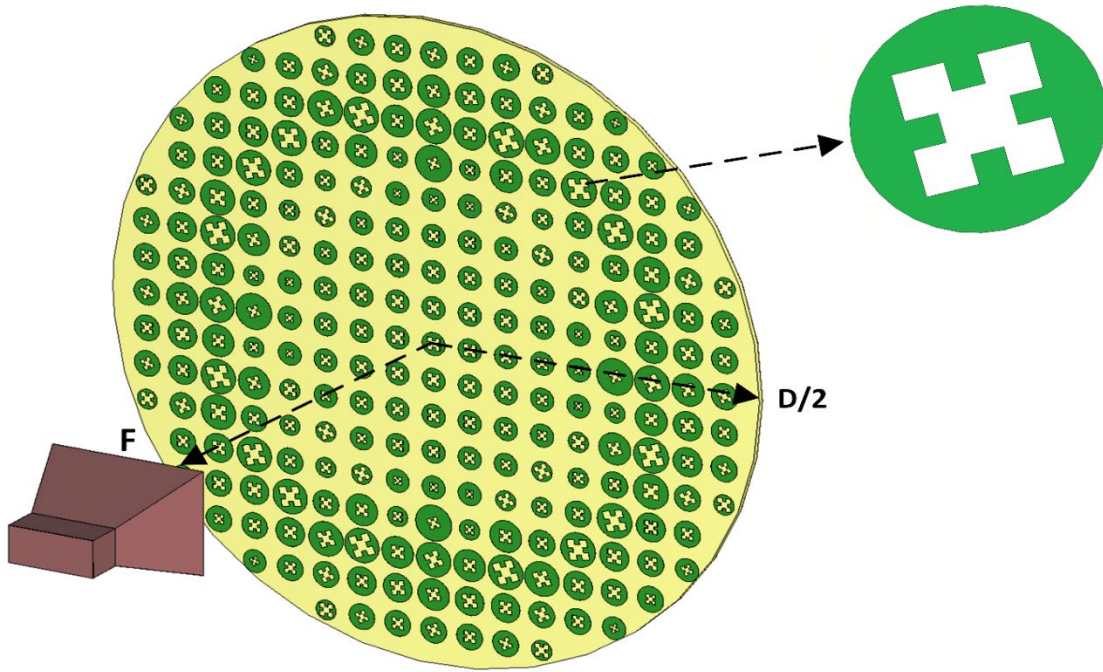
Figure 12. Reflective array antenna designed with Circle-Minkowski unit cells
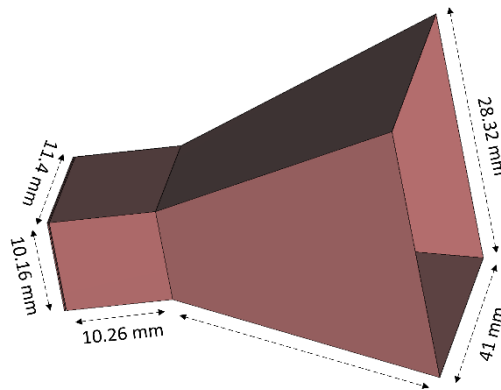

Figure 13. Horn antenna shape and dimensions

The phase response of all points on the RAA is provided with the unit cell obtained using the parameters and rotation angle of the Circle-Minkowski structure in Table 2, and accordingly, unit cells can be placed at all points on the RAA. After completing the design with RAA and horn antenna, the antenna is simulated with the help of electromagnetic simulation program. The gain of the horn antenna used here is 11.7 dBi. As a result of the simulated process, the gain graph shown in Figure 14 is obtained.
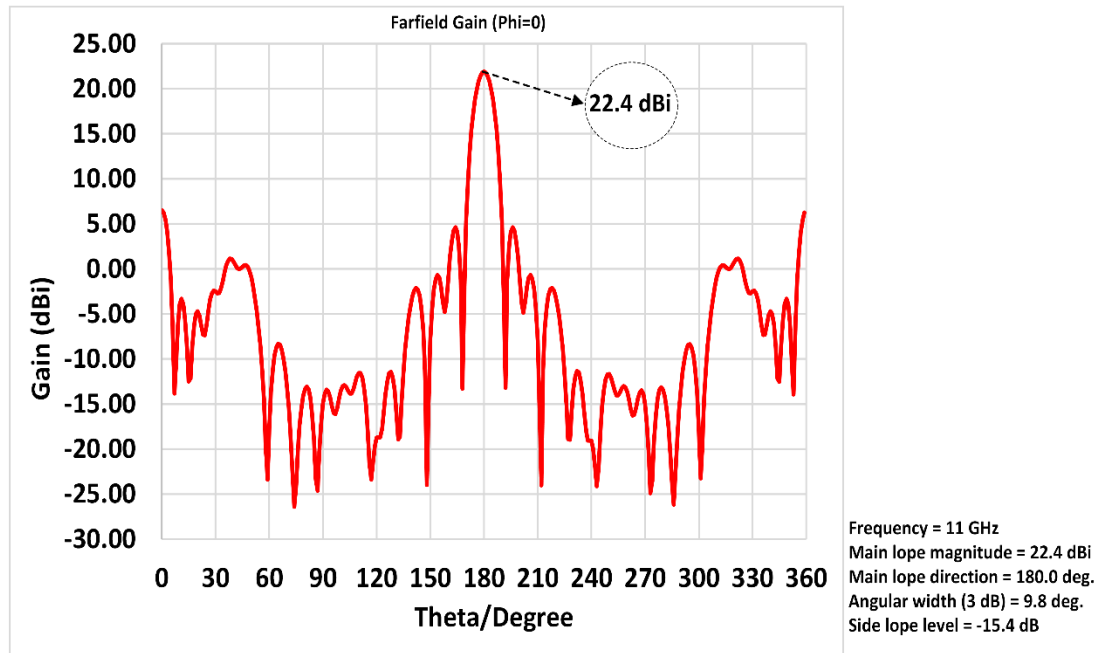
Figure 14. Gain graph of RAA

Figure 14 shows the cartesian gain graph. When the graphs are examined, it is seen that the maximum gain is 22.4 dBi and there is a good focus on the horn antenna.

3. RESULTS AND DISCUSSION

In this study, 3 different unit cell designs were made to be used on the reflective array antenna. First, the structure in Figure 1 was designed and simulated as a unit cell, and the reflection phase response was obtained depending on the circle diameter. According to the simulation results, the phase response of 280° was taken as seen in Figure 2. This means that phase response cannot be obtained throughout the entire band, and reflective unit cells cannot be placed at some points on the RAA to be formed depending on this situation. For this reason, the structure created by etching the Minkowski structure from the circle seen in Figure 3 was designed. While designing the Circle-Minkowski structure, there were three cases where two of the parameters m, t and s were kept constant and one of them was changed. For these three cases, 350 simulations were made using the parameter ranges given in Table 2 and a phase response of 329° was obtained. In the last step, the parameters of the circle-minkowski structure and the rotation of this structure for 10 angle values between 0°-30° were simulated and 3500 simulation processes were performed. As a result of the simulation, a phase response of 360° was obtained.

After the unit cell design, whose phase response can be obtained throughout the entire band, the antenna structure seen in Figure 11, created by placing a reflective unit cell at each point in the RAA formation, was simulated and the antenna gain at 11 GHz was obtained as 22.4 dBi. In addition, broadband antenna gain is given in Figure 15.
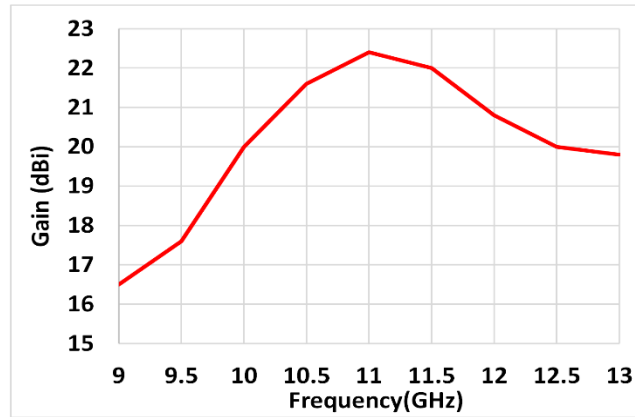
Figure 15. Wideband RAA gain graph

When Figure 15 is examined, it is seen that the antenna gain is 16.5 dBi for 9 GHz, 20 dBi for 10 GHz, 22.4 dBi for 11 GHz, 20.8 dBi for 12 GHz and 19.8 dBi for 13 GHz. Accordingly, it is seen that the antenna gain at 11 GHz is higher than the other frequencies.

4. CONCLUSIONS

In this study, it was first aimed to design a reflective unit cell with a wide phase response range. For this, a three-stage method was followed. Firstly, the reflective unit cell was simulated using a circular structure and the phase response of 280° was obtained as a result of the simulation. Then, in Stage 2, a new reflective unit cell was designed and simulated by etching the Minkowski structure from the circle structure. As a result of the simulation process according to the design parameters of the structure, 329° phase response was obtained. However, since the phase response could not be obtained for a full band, the last stage was started. At this stage, the Minkowski structure etched from the circle was rotated and simulated again, and a phase response of 360° was obtained. This allows adding a reflective unit cell to all points on the reflector array antenna, since phase response can be obtained over a full band. The RAA formed with these unit cells is shown in Figure 12. As a result of the simulation of the RAA, a gain of 22.4 dBi was obtained. Considering that the gain of the horn antenna is 11.7 dBi, a gain of 91% has been achieved compared to the gain of the horn antenna. According to these results, it has been revealed that a RAA design with wide phase range and high gain can be made by using the Circle-Minkowski structure by rotating effect.

REFERENCES

1. Genç, A.(2019). Gain Increase of Horn Antenna with Waveguide Feeding Network by using 3D Printing Technology. *Bayburt Üniversitesi Fen Bilimleri Dergisi*, Cilt 2, Sayı 1, Sayfa 17-25.

2. Genç, A., Başyiğit, İ. B., Çolak B., Helhel, S.(2018). Investigation of the characteristics of low-cost and lightweight horn array antennas with novel monolithic waveguide feeding networks, *AEU - International Journal of Electronics and Communications,* vol. 89, issue 1, pp 15-23.

3. Tütüncü, B., Urul, B. (2019). LHM superstrate for high directivity microstrip antenna", *Celal Bayar University Journal of Science*, vol. 15, issue 1, pp 71-74.

4. Gianvittorio, J.P., Rahmat-Samii, Y. (2002). Fractal antennas: a novel antenna miniaturization technique, and applications. *IEEE Antennas and Propagation Magazine*, vol. 44,no. 1, pp. 20–36.

5. Werner, D.H., Ganguly, S. (2003). An overview of fractal antenna engineering research. *IEEE Antennas and Propagation Magazine*, vol. 45, no. 1, pp. 38–57.

6. Costanzo, S., Venneri, F., Di Massa, G., Borgia, A., Costanzo, A., Raffo, A. (2016). Fractal reflectarray antennas: state of art and new opportunities. *Hindawi Publ.Corp.Int.J.of Antennas and Propagation*, vol. 2016, Art. ID 7165143, pp 17 http://dx.doi.org/10.1155/2016/7165143

7. Venneri, F., Costanzo, S., Di Massa, G., Amendola, G. (2008). Aperturecoupled reflectarrays with enhanced bandwidth features. *J. Electromagn. Waves Appl.*, vol. 22, pp. 1527–1537.

8. Al-Saedi, H., Abdel-Wahab, W.M., Raeis-Zadeh, S.M., Gigoyan, S., Safavi-Naeini, S. (2018). An Ultra-Wideband Modified Aperture-Coupled Millimeter-Wave Reflectarray Antenna. *IEEE International Symposium on Antennas and Propagation & USNC/URSI National Radio Science Meeting*, Boston, MA, USA, pp. 1423–1424, Jul.

9. Chaharmir, M.R., Shaker, J., Gagnon, N., Lee, D. (2010). Design of broadband, single layer dual-band large reflectarray using multi open loop elements. *IEEE Trans. Antennas Propagat.*, vol. 58, no. 9, pp. 2875–2883, Jun.

10. Li, L., Chen, Q., Yuan, Q., Sawaya, K., Maruyama T. (2009). Novel broadband planar reflectarray with parasitic dipoles for wireless communication applications. *IEEE Antennas Wireless Propag. Lett.*, vol. 8, pp. 881–885, Jul.

11. Yoon, J.H., Yoon, Y.J., Lee, W.S., So, J.H. (2015). Broadband microstrip reflectarray with five parallel dipole elements. *IEEE Antennas Wireless Propag. Lett.*, vol. 14, pp. 1109–1112, Jan.

12. Pozar, D.M. (2007). Wideband reflectarrays using artificial impedance surfaces. *Electron. Lett.*, vol. 43, no. 3, pp. 148–149, Feb.

13. Qin, P.Y., Guo, Y.J., Weily, A.R. (2016). Broadband reflectarray antenna using subwavelength elements based on double square meander-line rings. *IEEE Trans. Antennas Propag.*, vol. 64, no. 1, pp. 378–383.

14. Zubir, F., Rahim, M.K.A., Ayop, O., Wahid , A., Majid, H. A. (2010). Design and analysis of microstrip reflectarray antenna with minkowski shape radiating element. *Progress in Electromagnetics Research B*, vol. 24, pp 317–331.

15. Huang, J., Pogorzelski, R.J. (1998). A ka-band microstrip reflectarray with elements having variable rotation angles. *IEEE Transactions on Antennas and Propa.*, vol. 46, Issue 5, pp 650–656.

16. Lingasamy, V., Selvan, K.T. (2019). A comparison of planar convex dielectric lens loaded flat reflector with parabolic reflector and reflectarray. *Micr. and Optical Tech.Letters*, vol. 61 Issue 11, pp 2500-2505.

17. Keyghobad, K., Homayoon O. (2007). Phase Response of Microstrip Reflectarray Elements by FDTD Analysis. *Workshop on Computational Electromagnetics in Time-Domain, IEEE*, pp 1-3.